01,14

Molecular Dynamics Study of the Development of the Dislocation Structure of an FCC Crystal Containing an Ensemble of Spherical Pores under an External Force Action

© A.V. Markidonov[1], M.D. Starostenkov[2], V.N. Lipunov[2], D.A. Lubyanoy[3], P.V. Zakharov[4]

[1] Kuzbass Humanitarian Pedagogical Institute of Kemerovo State University, Novokuznetsk, Russia
[2] Polzunov Altai State Technical University, Barnaul, Russia
[3] Branch of T.F. Gorbachev Kuzbass State Technical University, Prokopyevsk, Russia
[4] Peter the Great Saint-Petersburg Polytechnic University, St. Petersburg, Russia

E-mail: markidonov_artem@mail.ru

Received January 25, 2023
Revised April 13, 2023
Accepted April 13, 2023

Radiation swelling is one of the most urgent problems in radiation materials science. Its successful solution requires an understanding of the features of the mechanisms of pore healing. In this regard, there are various experimental and theoretical works devoted to this topic. At present, due to the increase in the power of computing tools, computer simulation allows for more and more complex studies and is used, among other things, in the field of materials science. In this paper, we present the results of molecular dynamics simulations devoted to the study of the processes of healing of a group of spherical pores in an fcc crystal subjected to shear deformation. As the study showed, for pores located in close proximity to each other, the formation of a common dislocation loop is characteristic, which is formed as a result of the attraction of individual loops having sections with opposite signs of helical orientation. The formation and subsequent development of such a loop contributes to a decrease in the free volume localized in the crystal in the form of pores. In addition, structural transformations that occur when a shock wave is generated in the computational cell, which creates additional stresses, are considered separately. In this case, the formation of the loop described above and the subsequent collapse of individual pores are also observed. Taking into account that the simulation was carried out at temperatures insufficient to activate diffusion processes, and the temperature control procedure was used in model experiments with wave generation, we can conclude that the shock wave is the cause of pore collapse even in the absence of high temperatures, and one of the main mechanisms of this process is the development of the dislocation structure of the ensemble of pores.

Keywords: crystal, model, deformation, pore, dislocation.

DOI: 10.21883/PSS.2023.05.56037.10

1. Introduction

External impact on a crystalline body structure, for example, by accelerated particles, when energy is transmitted to lattice points, is followed by formation of stable radiation-induced defects. With sufficient vacancy supersaturation, vacancy clusters are formed as pores of various sizes. As a result of following coalescence in tendency to reduce free surface, larger pores are growing due to absorption of small pores, and a pore complex is formed [1,2]. In some cases, this phenomenon followed by an increase in the amount of irradiated material is totally unacceptable, therefore close attention is paid to radiation swelling control .

Taking into account a fact that a material is exposed to various power loads during operation, it is obvious that the arising stresses shall influence the vacancy cluster evolution process. Thus, [3–5] show that a pore is a source of dislocations generated under the influence of external stresses. Thus, strain regions confined in the form of dislocations are formed around pores and, in case of their intersection, pore coalescence occurs.

According representations addressed in classical Geguzins studies [6,7], pores are healed at moderate temperatures and applied stresses due to the growth of dislocations when emerging shear stresses overcome the threshold and a Frank−Read source is actuated. Formation of the dislocation loop results in dislocation of a pore boundary to the amount of the Burgers vector. Therefor, the extent of healing is defined by the number of generated dislocation loops. Power size is stabilized when the external impact has been compensated by stresses induced by the emitted dislocation loops.

Earlier, [8,9] addressed the dislocation loop generation on the surface of spherical and cylindrical pores under the in-

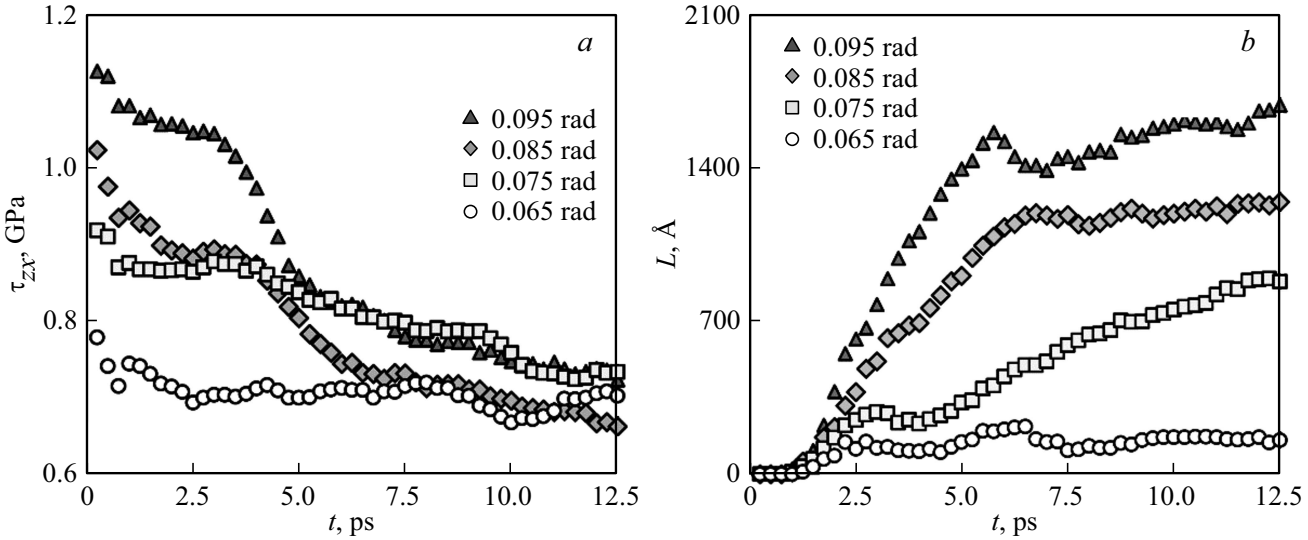

Figure 1. Variation of shear stresses and total length L of dislocation loops in a computational cell during simulation with various shear angles γ.

fluence of post-cascade shock waves and their subsequence healing. The goal of this study is to identify the mechanisms of pore complex healing in a strained crystal under the influence of shock waves.

2. Research procedure

Molecular dynamics computer simulation was chosen as the study method. This selection is based on the fact that the above method allows to track the dynamics of a system containing a sufficiently large amount of interacting particles with relatively low computational cost, and in future the obtained results may be compared with actual experiments, thus, overcoming one of the main computer simulation problems.

For calculations, a computational cell was built which simulated a FCC crystal and contained about 60 000 particles and whose infinite extension was achieved using periodic boundary conditions. Space orientation of cell axes corresponded to crystallographic directions $[1\bar{1}0]$, $[11\bar{2}]$ and $[111]$. Interparticle interaction was described using Johnson potential calculated within the embedded atom method [10]. The model parameters were selected for Au. Equations of motion describing the particle system behavior were integrated using Verlet velocity algorithm with time step 5 fs.

Pores in the computational cell were created by selecting spherical areas with various radii whose center coincided with the crystal lattice point followed by removal of the particles belonging to this area. Then the system relaxation was carried out and the resulting configuration reduced to the minimum potential energy was used for further investigation.

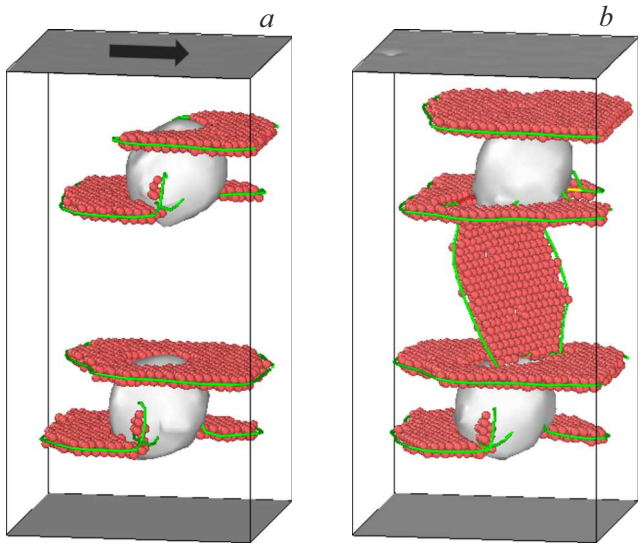

Figure 2. Dislocation structure visualization after 12.5 ps of simulation time with shear angles $\Gamma = 0.075$ (a) and 0.08 (b) rad. Atoms whose local environment corresponds to HCP lattice are shown. The arrow shows shear direction.

3. Simulation results

Consider a computational cell containing two pores with a radius of $4a_0$, where a_0 is the equilibrium lattice constant, which is susceptible to shear strain parallel to the lattice plane (111) along direction $[1\bar{1}0]$. This shear direction was selected, because, as shown in [8], stable formation of dislocation loops is observed in this case, which is of highest interest for the purpose of the study. After deformation of the computational cell, its geometry is retained using additional severe boundary conditions and then annealing

at the pre-defined temperature of 300 K is carried out. Such temperature does not allow initiation of pore diffusion processes and, therefore, enables the dislocation mechanism to be investigated. The completed calculations have shown that the shear stresses in the computational cell start to decrease which is indicative of current structural changes, and the greatest decrease is observed with the increase in the shear angle during a few picoseconds of simulation time (see Figure 1, *a*).

Structure visualization carried out by means of third-party software [11] has demonstrated formation of dislocation shear loops located in the family planes on pores {111} (see Figure 2). For such imaging process, a free surface was selected within the computational cell, i.e. a pore, atoms whose local environment is other than FCC (stacking faults) and dislocation lines defines using DXA algorithm

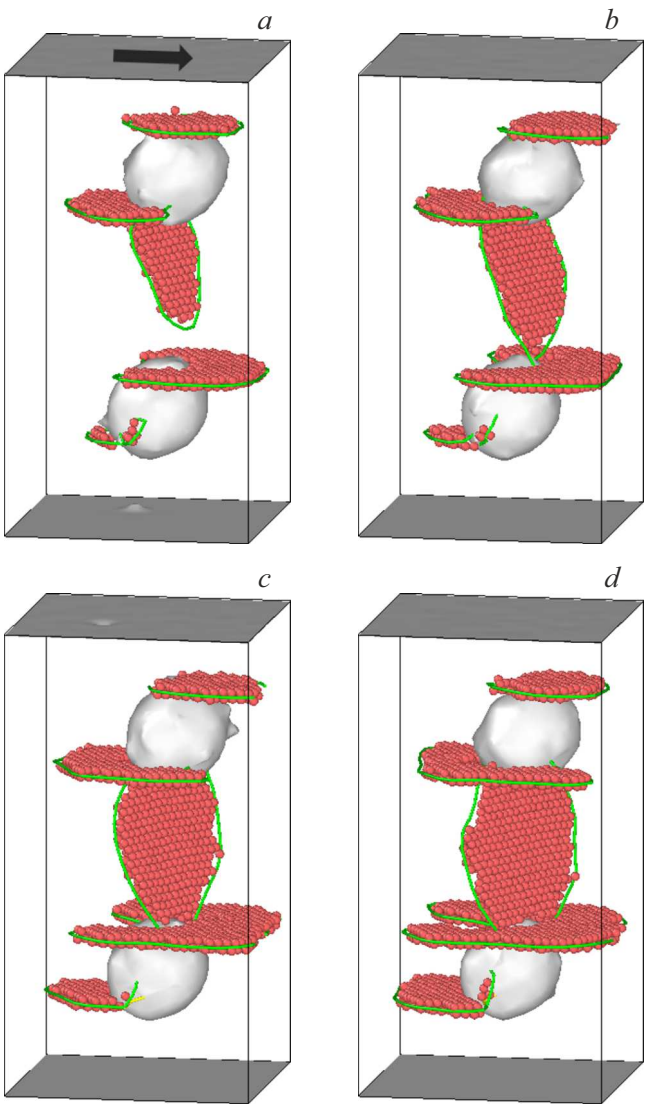

Figure 3. Dislocation structure visualization after 4.5 (*a*), 5 (*b*), 6.25 (*c*) and 7.5 (*d*) ps of simulation time with shear angle $\gamma = 0.08$ rad.

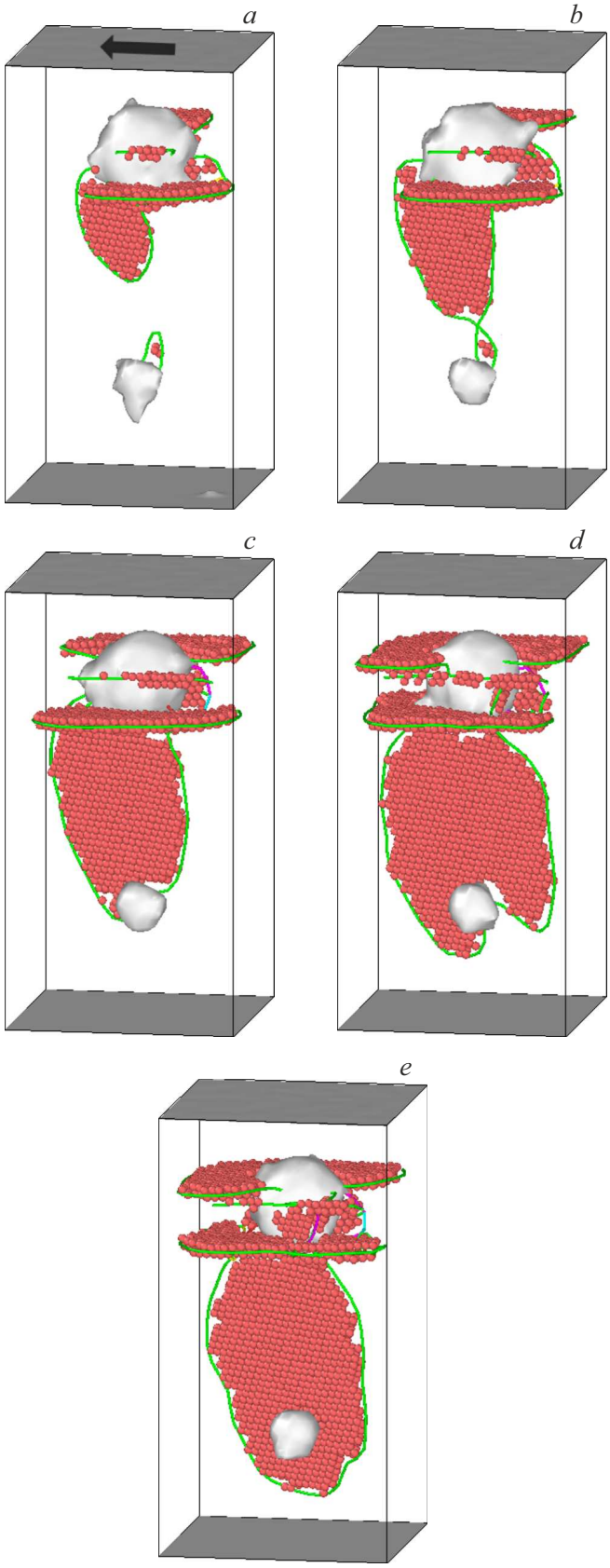

Figure 4. Dislocation structure visualization after 4.75 (*a*), 5.75 (*b*), 7.5 (*c*), 12 (*d*) and 15 (*e*) ps of simulation time with shear angle $\gamma = 0.085$ rad and pores of different sizes.

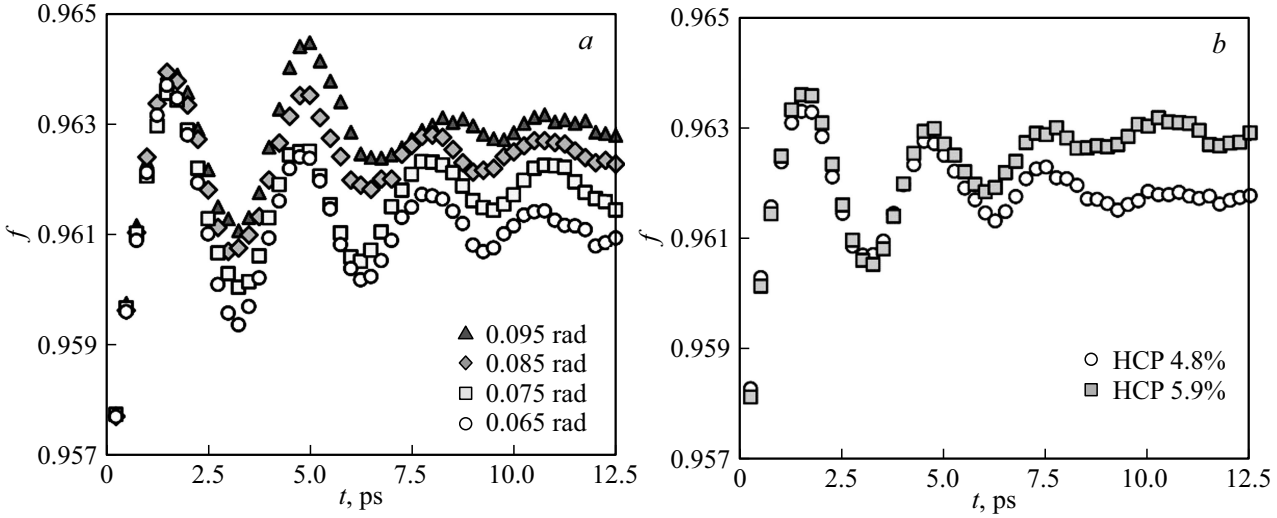

Figure 5. Variation of volume fraction of a„phase of matter“ f with various shear angles γ (a) and various dislocation structure development (b) (shear angle $\gamma = 0.08$ rad).

(dislocation extraction algorithm) [12]. This algorithm was additionally used to calculate a total length of dislocation lines identified in the computational cell, which allowed to evaluate the dislocation structure development with various shear angles (see Figure 1, b).

As shown in Figure 2, b, with shear angle $\gamma = 0.08$ rad, a dislocation loop adjacent to both pores is formed. More detailed investigation has shown that, in this case, the shear loop initiated on the surface of one of the pores gradually increases in sizes, however, unlike other formed loops after overcoming the critical position, in terms of the Frank–Read source, it does not expand around the point of formation, but rather extends towards the surface of the adjacent pore (See Figure 3).

Similar pore complex interaction process is also observed with other radii of simulated pores (See Figure 4). In this case, dislocation loops are formed, which have segments with opposite screw orientation signs. Thus, they are attracted, annihilate and form a common loop which continues to expand and intersects a smaller pore (in this case, with radius $2a_0$).

The created shear strain followed by dislocation structure development results in reduction of the free computational cell volume confined in the form of pores. A free surface identification algorithm described in [13] was used to evaluate the free volume. However, from our point of view, it is more suitable to evaluate the volume occupied by the system particles vs. total volume of the computational cell that will be hereinafter referred to as the specific volume of a „phase of matter“ f [9].

The investigation has shown that f grows with shear angle growth (see Figure 5, a).

By increasing the distance between pores, a situation can be achieved when a loop enclosing them is not formed. Thus, the dislocation structure is less developed and f is lower (see Figure 5, b). In this case, development of the dislocation structure is evaluated using a fraction of atoms whose local environment corresponds to HCP lattice.

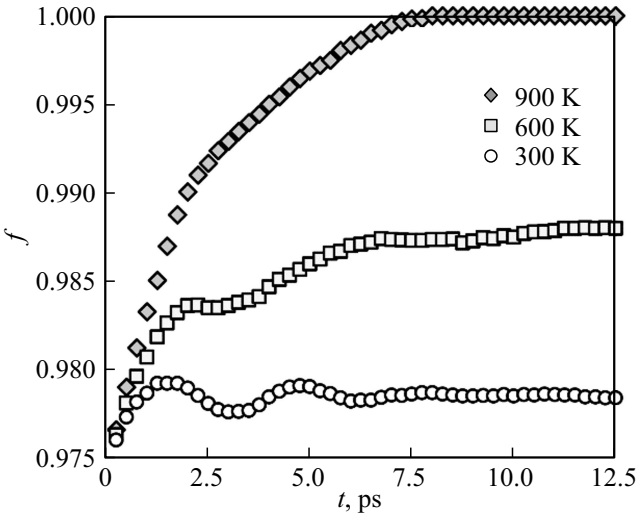

Figure 6. Change of volume fraction of a „phase of matter“ f at various computational cell temperatures (shear angle $\gamma = 0.075$ rad, pores of various sizes).

Therefore, it may be concluded that formation of a common dislocation loop enclosing a pore complex contributes significantly to the process of reduction of a free volume confined in the crystal.

If the computational cell temperature is additionally increased, then diffusion processes are initiated and pores start to dissolve. For clarity, Figure 6 shows calculations of f at different temperatures of the computational cell containing a pore complex with radius $4a_0$ and $2a_0$. In this case, at initial temperature $T_0 = 600$ K, dissolution of a pore with the smallest radius is observed, and both pores are dissolved at $T_0 = 900$ K and f becomes equal to 1.

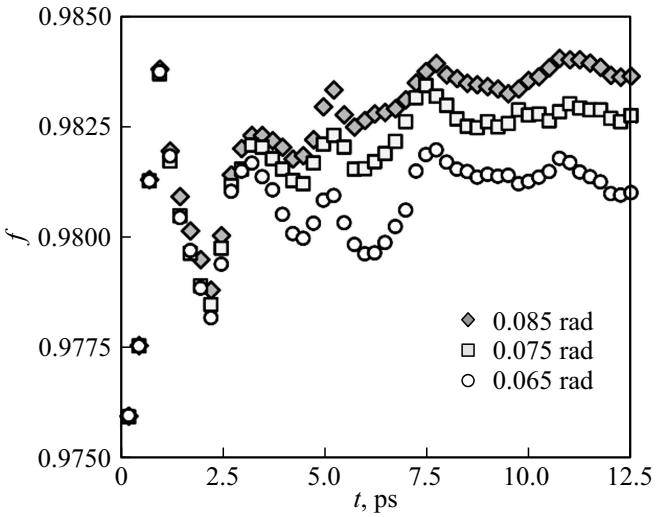

Figure 7. Change of volume fraction of a „phase of matter" f at various shear angles γ in case of shock wave generation in the computational cell (pores of various sizes).

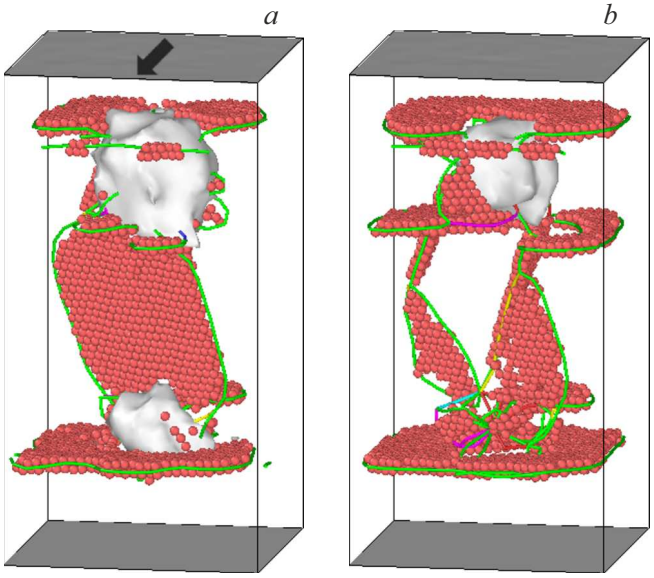

Figure 8. Dislocation structure visualization after 5.5 (a) and 14.25 (b) ps of simulation time with shear angle $\gamma = 0.085$ rad and pores of different sizes in case of shock wave generation in the computational cell.

Earlier the authors of [14,15] showed that a shock wave created in the computational cell results in various changes of the faulted structure of the simulated crystal and induces additional shear stresses [16]. Therefore, investigation of the shock wave impact on the pore complex is of interest. Procedure for creation of such wave within a molecular dynamic model is described, for example, in [14]. However, it should be noted that a temperature control procedure is used to avoid heating of the computational cell.

The investigation has shown that the shock wave induced in the computational cell leads to reduction of a free volume by means of pore collapse, which is achieved due to the growth of shear stresses, rather than temperature growth as in case shown in Figure 6. Thus, Figure 7 shows variation of f at various shear angles when a shock wave is induced. Growth of f at shear angles 0.075 and 0.085 rad is due to a small pore collapse (radius $2a_0$) in 11 and 6.25 ps, respectively.

Structural analysis of the computational cell has shown that the wave initiates more intense development of dislocation shear loops (see Figure 8, a) compared with previous simulation experiments (see Figure 7 for comparison). In this case, after pore collapse in the computational cell, structural transformations continue and Lomer–Cottrell disclocations are formed (see Figure 8, b).

4. Conclusions

The investigation has shown that formation of a dislocation loop enclosing the pores as a result of interaction between individual loops initiated on the pore surfaces under the influence of shear strain is one of the main pore healing mechanism for pores positioned side-by-side. Moreover, formation of such loop under the shock wave impact may cause collapse of some pores even at temperatures insufficient for initiation of diffusion processes.

Conflict of interest

The authors declare that they have no conflict of interest.

References

[1] V.L. Orlov, A.G. Malyshkina, A.V. Orlov. Izv. Tomskogo politekhnicheskogo un-ta. **305**, *3*, 314 (2002). (in Russian).
[2] P.N. Ostapchuk. Voprosy atomnoy nauki i tekhniki **9**, 2012 (2003). (in Russian).
[3] Q. Xu, W. Li, J. Zhou, Y. Yin, H. Nan, X. Feng. Comput. Mater. Sci. **171**, 109280 (2020).
[4] Y.-L. Guan, J.-L. Shao, W. Song. Comput. Mater. Sci. **161**, 385 (2019).
[5] C.J. Ruestes, E.M. Bringa, A. Stukowski, J.F. Rodriguez Nieva, Y. Tang, M.A. Meyers. Comput. Mater. Sci. **88**, 92 (2014).
[6] Ya.E. Geguzin, V.G. Kononenko, V.T. Tchan. Poroshkovaya metallurgiya, **2**, 26 (1976). (in Russian).
[7] Ya.E. Geguzin, V.G. Kononenko. Fizika i khimiya obrabotki materialov **60**, 1982 (2021). (in Russian).
[8] A.V. Markidonov, M.D. Starostenkov, P.V. Zakharov, D.A. Lubyanoy, V.N. Lipunov. ZhETF **156**, *6*, 1078 (2019). (in Russian).
[9] A.V. Markidonov, M.D. Starostenkov, D.A. Lubyanoy, P.V. Zakharov, V.N. Lipunov. Izv. vuzov. Chernaya metallurgiya, **64**, 427 (2021). (in Russian).

[10] R.A. Johnson. Phys. Rev. B **39**, *17*, 12554 (1989).
[11] A. Stukowski. Mod. Simul Mater. Sci. Eng. **18**, 015012 (2010).
[12] A. Stukowski, K. Albe. Mod. Simul Mater. Sci. Eng. **18**, *8*, 085001 (2010).
[13] A. Stukowski. JOM **66**, *3*, 399 (2014).
[14] A.V. Markidonov, P.V. Zakharov, M.D. Starostenkov, N.N. Medvedev. Mekhanizmy kooperativnogo povedeniya atomov v kristallakh. Novokuznetsk (2016). 220 p. (in Russian).
[15] M.D. Starostenkov, A.V. Markidonov, P.V. Zakharov, P.Y. Tabakov. Met. Mater. Res. Foundations **63**, 184 (2019).
[16] M.D. Starostenkov, A.V. Markidonov, P.Y. Tabakov. Deformatsiya i razrushenie materialov, **6**, 2 (2016). (in Russian).

Translated by E.Ilyinskaya